

Synthesis and Characterization of Functionalized Platinum Nanoparticles

H. Perez,^{*,†} J.-P. Pradeau,[†] P.-A. Albouy,[‡] and J. Perez-Omil^{†,§}

CEA DSM/DRECAM, Service de Chimie Moléculaire, Bât. 125, 91191 Gif s/Yvette, France, and Laboratoire de Physique des Solides (U.M.R. 8502), Bât. 510, Université de Paris-Sud, 91405 Orsay, France

Received February 1, 1999. Revised Manuscript Received September 2, 1999

The elaboration and characterization of platinum nanoparticles functionalized with 4-mercaptoaniline is reported. An important point of the synthesis scheme is the use of hexylamine as intermediate labile capping agent. The size and structure of the platinum inner core have been analyzed by X-ray diffraction and TEM microscopy. It is found to be crystalline with a fcc structure and a cell parameter of 0.392 nm very close to the bulk value. The size dispersity is low with an average diameter of ca. 1.5 nm. A well-defined interparticle distance of ca. 3.2 nm is found, corresponding to an organic overlayer thickness of 0.9 nm in good agreement with the estimated molecule length. A rough estimation of the surface per absorbed molecule yields a value of ca. 0.14 nm², pointing to a dense molecular packing. However, IR spectroscopy reveals a very slow degradation process of the organic overlayer, eventually resulting in the formation of sulfate ions onto the platinum surface. A promising perspective is the use of the amine end groups for subsequent overgrafting of the nanoparticles.

1. Introduction

The synthesis and characterization of functionalized nanoparticles is currently a very active field of research. Capping nanoparticles with bifunctional molecules allows the introduction of a variety of chemical reactivities at the outer surface.^{1–4} This reactive interface is of prime importance as it links minerals and organics and opens fascinating possibilities toward building versatile nanocomposite architectures. Indeed, it could play various roles within the nanocomposite architecture: promoting a peculiar ordering, inducing some specific properties within the assembly or creating synergies between specific properties of the particles and the capping organic molecules.

In the present publication we report on a synthesis of platinum nanoparticles which allows easy functionalization using 4,4'-diaminodiphenyl disulfide. The functionalized particles are characterized by infrared spectroscopy, X-ray diffraction, transmission electron microscopy, and elemental analysis.

2. Experimental Section

2.1. Materials. Hexylamine, sodium borohydride (NaBH₄) 99%, 4,4'-diaminodiphenyl disulfide 98%, and platinum(IV)

chloride (PtCl₄) 99.99% were obtained from Aldrich and used as received. PtCl₄ was stored in a desiccator under vacuum.

2.2. Synthesis. A 300 mg sample of PtCl₄ is dissolved in 75 mL of hexylamine in a 500 mL flask to give an orange solution (solution 1). Then, 330 mg of 4,4'-diaminodiphenyl disulfide is dissolved in 30 mL of a methanol/hexylamine solution (50/50) (solution 2). Finally, 300 mg of NaBH₄ is dissolved in 40 mL of a water/methanol solution (50/50); just after complete dissolution of sodium borohydride, hexylamine (20 mL) is added (solution 3). Solution 3 is then poured into solution 1 under vigorous stirring at room temperature. The reaction mixture turns brown within a few seconds, and after 20 s, solution 2 is added to the reaction mixture. After 3.5 min, 200 mL of pure water is added, and the resulting solution is stirred for 15 min before being transferred into a separatory funnel. Just after phase separation, the water is removed and the organic phase is repeatedly washed with the same amount of water (200 mL). The volume of the dark brown organic phase is reduced to ca. 3–4 mL by rotary evaporation at about 35 °C and transferred into a centrifuge tube with 0.3 g of disulfide dissolved in 15 mL of ethanol. After this solution is stirred overnight, a black solid residue is recovered by centrifugation. The supernatant presumably contains unreacted disulfide and platinum complexes. The precipitate is washed either with pure ethanol or with diethyl ether and centrifuged again. The use of ethanol allows the separation of two fractions exhibiting different size distributions (see below, X-ray characterization): fraction 1 is the precipitate, and fraction 2 is recovered from the dark brown supernatant after treatment with a large excess of diethyl ether. The total mass thus obtained is 90 mg, the proportion between the two fractions being variable. About 18 wt % corresponds to organic material grafted onto the particles (see below elemental analysis), and the reaction yield calculated with respect to platinum is ca. 40%. Both fractions readily dissolve in dimethyl sulfoxide, yielding dark brown solutions which remain stable for several weeks.

2.3. Characterization. Infrared spectra were recorded with KBr pellets using a 1720 X Perkin-Elmer FTIR spectrometer (2 cm⁻¹ resolution).

* To whom correspondence should be addressed.

† Service de Chimie Moléculaire.

‡ Université de Paris-Sud.

§ On leave from Dpto. Ciencia de Materiales, Universidad de Cadiz, Apdo. 40, 11510-Puerto Real, Spain.

(1) Noglik, H.; Pietro, W. *Chem. Mater.* **1994**, *6*, 1593.

(2) Brust, M.; Fink, J.; Bethell, D.; Schiffrin, D. J.; Kiely, C. *J. Chem. Soc., Chem. Commun.* **1995**, 1655.

(3) Buining, P. A.; Humbel, B. M.; Philipse, A. P.; Verkleij, A. J. *Langmuir* **1997**, *13*, 3921.

(4) Templeton, A. C.; Hostetler, M. J.; Kraft, C. T.; Murray, R. W. *J. Am. Chem. Soc.* **1998**, *120*, 1906.

Table 1. Pertinent Parameters Obtained from X-ray Diffraction Analysis

	inter-particle distance (nm)	correlation distance (nm)	3a/4a ratio (%)	averaged particle size (nm)	organic layer thickness (nm)
synthesis I					
fraction 1	3.17	6.8	15/85	1.50	0.84
fraction 2	3.22	7.5	58/42	1.38	0.92
synthesis II					
fraction 1	3.28	6.1	10/90	1.60	0.84
fraction 2	3.34	7.0	50/50	1.37	0.98
synthesis III					
fraction 2 ^a	3.34	7.6	52/48	1.36	0.99

^a Fraction 1 not analyzed.

X-ray measurements are conventionally performed on a θ - 2θ goniometer in reflection geometry using pressed tablets as samples.⁵ However, this procedure is excluded in the present case due to the very small amount of matter available. Diffraction diagrams were recorded in a transmission geometry on photostimulable imaging plates or with a position-sensitive detector using 0.3 mm glass capillaries. In this way, the amount of necessary material does not exceed 1 mg with exposure times of a few hours. The X-ray source was a rotating anode generator equipped with a doubly curved graphite monochromator (copper anode; small focus).

Electron microscopy images were obtained with a Philips EM430 TEM microscope operating at 300 kV. The samples were prepared by allowing a few drops of a dimethyl sulfoxide/chloroform solution to evaporate on carbon-coated copper grids.

3. Results and Discussion

3.1. Synthesis. The synthesis presented here uses hexylamine as the intermediate labile capping agent. The final capping agent is introduced in the reaction mixture only after reduction of the platinum salt. This strategy is dictated by preliminary experiments suggesting that platinum reduction in the presence of disulfide is a much slower process: in this case, sodium borohydride addition does not result in the rapid appearance of the dark brown color characteristic of the formation of platinum nanoparticles. The rapid addition of disulfide after platinum reduction is necessary to prevent irreversible particle flocculation but is probably responsible for the relatively low reaction yield. The flocculation is due to several factors, including the weak interaction of amine functions with platinum surface and the concentration of platinum salt in the reaction mixture. Similarly, it has been suggested that the stability of amine-capped gold particles is largely more kinetic than thermodynamic in nature.⁶

Before centrifugation an overnight treatment with an excess of disulfide is performed to optimize particle coverage.

Elemental analysis performed on synthesis III, fraction 2 (see Table 1) yielded Pt, 82.1%; C, 8.2%; S, 4.3%; N, 1.5%; H, 0.7% by weight, and 3.2% of the total mass is lacking and is attributed to oxygen. This point is discussed below.

3.2. Infrared Spectroscopy. IR spectra of fraction 1 and 2 are shown in Figure 1. Both fractions exhibit the same spectrum where characteristic absorption

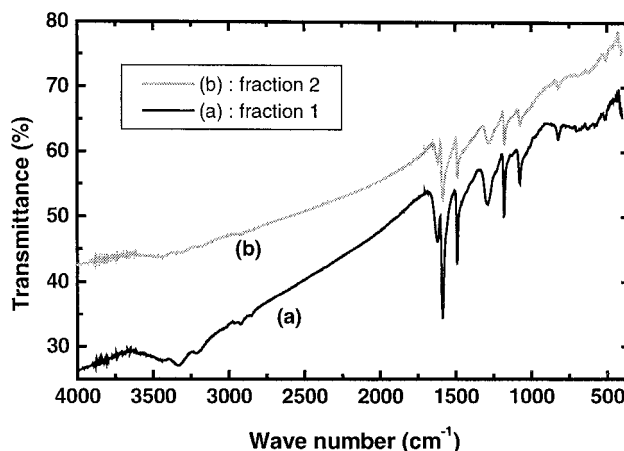


Figure 1. Infrared spectra of platinum nanoparticles functionalized with 4-thioaniline: (a) fraction 1; (b) fraction 2.

bands of the bifunctional molecule appear. The very tiny peak at ca. 2900 cm^{-1} is due to residual hexylamine. Absorption peaks above 3000 cm^{-1} are attributed to N-H stretching modes whereas the peak located at 1615 cm^{-1} is characteristic of NH_2 deformation. The C-N stretching mode is probably located at 1278 cm^{-1} . The aromatic ring exhibits vibrations at 1581 and 1484 cm^{-1} (aromatic ring stretching modes). Absorption involving C-H bonds is found at 1175 cm^{-1} (in-plane bending modes) and 816 cm^{-1} (C-H wagging vibration). The location of these vibrations is characteristic of para-disubstituted benzene.⁷

We observed additional bands located at 1340, 1125, 1002, and 945 cm^{-1} when washing of the organic phase with water is insufficient. They are probably due to borate species which are side products of sodium borohydride.^{7,8}

The infrared spectra of the product were recorded as a function of time and point to a chemical evolution characterized by the slow elimination of the organic capping molecules. This process is completed within several months as illustrated by the comparison of curves a and b in Figure 2 corresponding respectively to freshly prepared powders and samples kept 4 months in air. This evolution is characterized by the disappearance of the absorption lines of 4-mercaptoaniline and the apparition of new absorption peaks located at 1107 and 617 cm^{-1} . They can be attributed to ν_3 and ν_4 infrared-active modes of SO_4^{2-} anions, which are the final product of the chemical degradation. The rupture of the S-C bond and subsequent elimination of aniline can therefore be suspected. This could explain the loss of nitrogen and presence of oxygen indicated by elemental analysis. On the basis of the sulfur-to-platinum ratio, the empirical formula of the freshly synthesized nanoparticles is tentatively written as $\text{Pt}_{3.4}(\text{SC}_6\text{H}_4\text{NH}_2)$.

3.3. X-ray Diffraction. The diffractograms represented on Figure 3 have been obtained by imaging plates scanning or with a position sensitive detector and cover an angular domain extending from ca. 1° to 90° in 2θ . The wide-angle zone is dominated by a series of

(5) Gnutzmann, V.; Vogel, W. *J. Phys. Chem.* **1990**, *94*, 4991. Rodriguez, A.; Amiens, C.; Chaudret, B.; Casanove, M.-J.; Lecante, P.; Bradley, J. S. *Chem. Mater.* **1996**, *8*, 1978.

(6) Leff, D. V.; Brandt, L.; Heath, J. R. *Langmuir* **1996**, *12*, 4723.

(7) Colthup, N. B.; Daly, L. H.; Wiberley, S. E. In *Introduction to Infrared and Raman Spectroscopy*, 3d ed.; Academic Press: San Diego, CA, 1990.

(8) Nakamoto, K. In *Infrared and Raman Spectra of Inorganic and Coordination Compounds*, 5th ed.; John Wiley & Sons: New York, 1997.

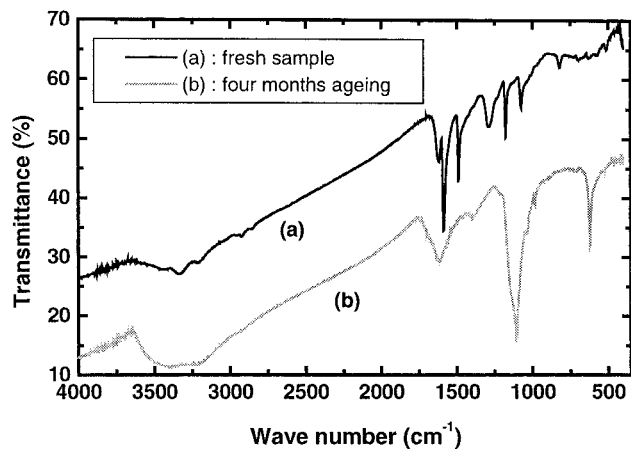


Figure 2. Infrared spectra of freshly synthesized nanoparticles functionalized with 4-thioaniline (a) and after 4 months evolution in air (b).

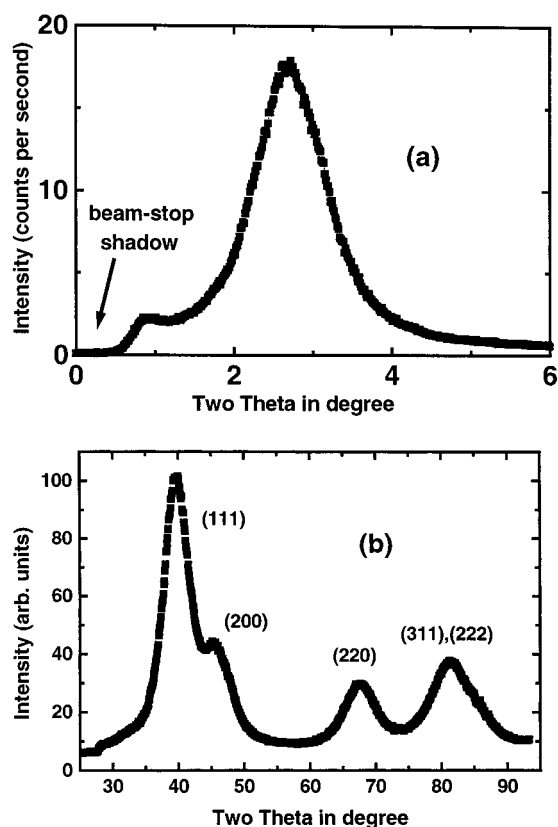
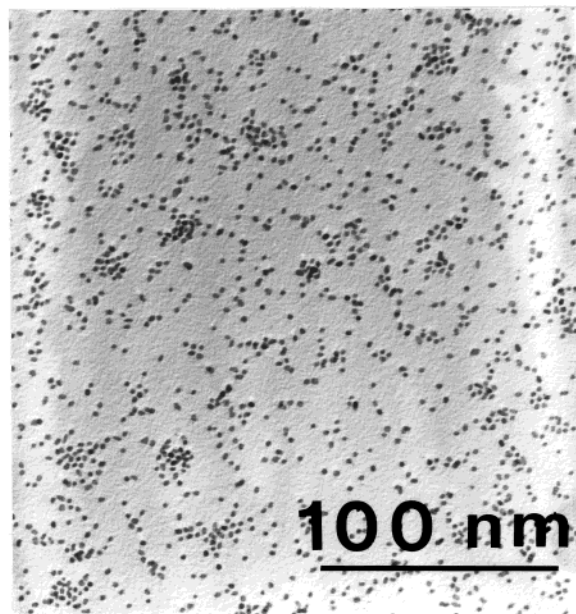
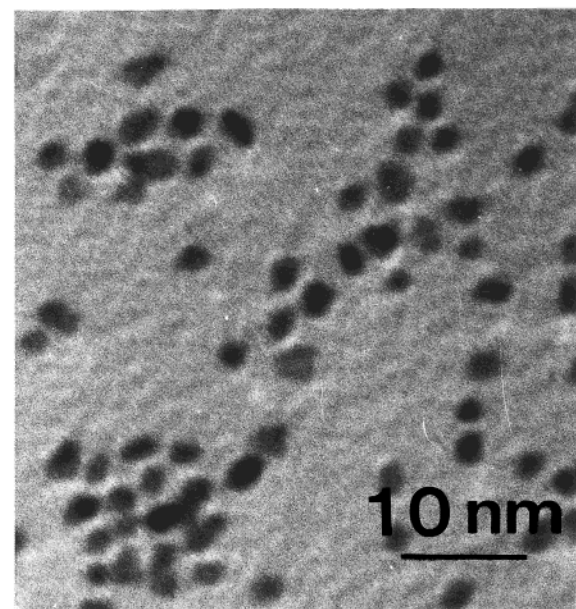


Figure 3. (a) Small-angle diffraction pattern recorded with a position sensitive linear detector (recording time, 10 min; sample from synthesis II, fraction 1). (b) Wide-angle X-ray diffraction pattern obtained by imaging plate scanning. Indexing corresponds to an fcc structure (exposure time, 5 h; sample from synthesis I, fraction 1).

broad lines due to intraparticle diffraction (Figure 3b) whereas the intense peak observed at a smaller angle is related to the interparticle packing distance (Figure 3a). Some determinations of this distance are given in Table 1 for different preparations together with an estimation of the associated correlation distance (evaluated from the angular peak width using the Scherrer formula⁹): as shown in Table 1, the correlation distance is typically twice the interparticle distance, which means that positional correlations do not extend over more than second neighbors.



a



b

Figure 4. (a, b) TEM images obtained at different magnifications from platinum particle/dimethyl sulfoxide solutions evaporated on carbon grids (sample: synthesis II, fraction 2; see Table 1).

The clear separation of the large-angle diffraction lines points to a fcc structure of the particles in majority.⁵ We faced two problems which dissuaded us from trying to fit systematically the whole diffraction diagram with Debye functions.^{5,9} In some cases, the amount of matter was so minute that recording the weaker diffraction lines was very tedious, and in other cases the irregular shape of the sample precluded any reliable correction for absorption. We adopted a simplified procedure consisting in an adjustment of the profile of the more intense (111) reflection with Debye functions

(9) Klug, H. P.; Alexander, L. E. In *X-ray Diffraction Procedures for Polycrystalline and Amorphous Materials*; John Wiley & Sons: New York, 1954; p 491.

calculated for aggregates cubic in shape. In every case, a satisfactory agreement could be obtained using particles of edges $3a$ and $4a$, where a is the cubic parameter: at the precision of the present measurements, this parameter is equal to the bulk value (0.392 nm to compare to the bulk parameter 0.3924 nm). Percentages for different preparations are given in Table 1: fraction 2 (recovered from the supernatant) contains a higher proportion of smaller particles whereas fraction 1 mainly contains $4a$ particles.

The thickness of the organic overlayer is obtained from the difference between the interparticle distance and the particle average diameter. Determinations listed in Table 1 average to 0.9 nm in good agreement with the estimated length of 4-thioaniline including Pt–S bond. Elemental analysis data (see section 3.1) can be combined to X-ray diffraction results to estimate the particle coverage. Particles corresponding to the empirical formula $\text{Pt}_{3.4}(\text{SC}_6\text{H}_4\text{NH}_2)$ exhibit a $3a/4a$ ratio of 52/48 (see Table 1). This ponderation leads to ca. 265 platinum atoms per particle, i.e., ca. 79 chemisorbed molecules for an average surface of 11.4 nm^2 (with the assumption of particles cubic in shape). It results in a surface of 0.14 nm^2 per adsorbed molecule. This rough estimation is to be compared with the estimated molecular cross section of 4-thioaniline (ca. 0.2 nm^2) and points to a close packing of the molecules onto the platinum surface.

3.5. Electron Microscopy. Illustrative photographs obtained by TEM are given in parts a and b of Figure 4. The low size polydispersity is best illustrated by Figure 4a corresponding to fraction 2 of synthesis II (magnification: 260 000). A picture analysis allows a histogram of the platinum particle size to be drawn (see Figure 5). It essentially reflects the existence of two populations with diameters of ca. 1.5 nm (65%) and 1.8 nm (25%). This result is in correct agreement with our treatment of X-ray data leading to a 50–50 proportion of particles with edges $3a$ – $4a$ (see Table 1). Figure 4b is a 5-fold magnification of Figure 4a, showing the existence of a well-defined interparticle distance. A value of 3.5 nm is found, in good agreement with X-ray results (3.34 nm). Indeed, the above given distances and sizes must be taken as indicative in regard to the slightly oblate shape of most particles.

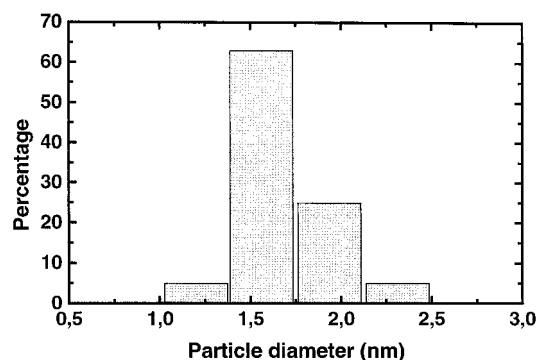


Figure 5. Size distribution of the platinum nanoparticles derived from an analysis of the TEM image in Figure 4a.

4. Conclusions

4-Thioaniline-functionalized platinum nanoparticles have been obtained by reduction of PtCl_4 using hexylamine as intermediate capping agent. This synthesis allows two fractions with different particle sizes to be separated. In every case the particle population is satisfactorily described as a mixture of cubic aggregates with $3a$ and $4a$ edges. It is further shown that the coverage of the particle by 4-thioaniline is quite dense. This feature is corroborated by the fact that the thickness of the organic overlayer is in good agreement with the estimated molecule length.

The high density of amine functions offers the possibility of overgrafting the particles by various molecules. Preliminary experiments have successfully tested this assumption.¹⁰ Furthermore, we are currently investigating the electrical properties of nanocomposite architectures built from such particles using the Langmuir–Blodgett technique.

Acknowledgment. We would like to thank P. Dubuisson and A. Kilenkembo for TEM photographs and Prof. M. P. Pileni for useful comments on the present paper (CEA Saclay, CEREM SRM and SRSI laboratories, Paris VI University).

CM991013I

(10) Perez, H.; Pradeau, J.-P.; Albouy, P.-A. To be published.